inorganics

MDPI

Article

Silver Nanoparticle-Immobilized Cotton Fabric Serves as Flexible Surface-Enhanced Raman Scattering Substrate for Detection of Toxin

Bharat Baruah * and Michael Woods

Department of Chemistry and Biochemistry, Kennesaw State University, Kennesaw, GA 30144-5591, USA; woods475@umn.edu

* Correspondence: bbaruah@kennesaw.edu; Tel.: +1-470-578-2654; Fax: +1-470-578-9137

Abstract: We designed composite materials containing silver nanoparticles (AgNPs) and cotton fabric (CF). The cellulose in cotton fabric contains -OH groups. These -OH groups were deprotonated by a pretreatment process, and Ag^+ ions were allowed to bind. In the consecutive step, the Ag^+ ions were reduced to fiber-bound AgNPs, generating AgNP@CF. Three different AgNP@CF composites were created, varying the concentration of the precursor $AgNO_3$ solution. The composite materials were characterized by scanning electron microscopy (SEM), energy-dispersive X-ray analysis (EDX), powder X-ray diffraction (XRD), and FTIR spectroscopy. The AgNP@CF composites were assessed for the detection of toxins using the surface-enhanced Raman scattering (SERS) technique.

Keywords: cellulose fiber; silver nanoparticles; toxins; SERS; analyte

Citation: Baruah, B.; Woods, M. Silver Nanoparticle-Immobilized Cotton Fabric Serves as Flexible Surface-Enhanced Raman Scattering Substrate for Detection of Toxin. *Inorganics* **2024**, *12*, 170. https://doi.org/10.3390/inorganics12060170

Academic Editor: David Morales-Morales

Received: 16 May 2024
Revised: 6 June 2024
Accepted: 11 June 2024
Published: 17 June 2024

1. Introduction

Various analytical techniques have been used in recent years for rapid and sensitive detections of toxins [1], such as gas chromatography–tandem mass spectrometry (GC-MS/MS) [2], high-performance liquid chromatography (HPLC) [3], and enzyme-linked immunosorbent assay (ELISA) [4]. These conventional methods require a relatively longer sample preparation time and expensive instruments. In food safety testing, the most frequently used analytical methods are gas chromatography (GC), liquid chromatography (LC), and capillary electrophoresis (CE) [5]. Later, the separated compounds are identified by near-infrared (NIR) spectroscopy, UV–visible spectroscopy, nuclear magnetic resonance (NMR), and mass spectroscopy (MS) [6,7]. Infrared spectroscopy and Raman spectroscopy are based on molecular vibrations. However, the latter one is immune to the interference from moisture in the sample, allowing for the superior detection of analytes [8].

Surface-enhanced Raman scattering (SERS) has been finding its way in the analytical realm due to its high sensitivity, non-invasiveness, unique spectroscopic fingerprint, and rapid results [9,10]. The advantage of SERS over traditional Raman spectroscopy is the electromagnetic enhancement due to the local surface plasmon resonance on the nanostructured noble metal and charge transfer between the analyte molecule and the noble metal surface [11]. Considering the above advantages, SERS is a frequently used analytical technique for food safety [12], homeland security [13], biomedicine [14], and environmental monitoring [15]. Traditional SERS substrates involve the deposition of metal nanoparticles, such as silver (Ag), gold (Au), copper (Cu), etc., on surfaces like glass and silicon wafers [16,17]. The detection of non-planar solid samples needs modification with such solid substrates [18]. For this reason, flexible substrates such as polymer films, cotton fabrics, papers, adhesive tape, and biomaterials have been gaining much attention as flexible SERS substrates, as they allow for favorable sample collection from any real-world surfaces [19,20].

Utilizing flexible SERS substrates has several advantages. They are easy to trim to any preferred size and shape, and the sample surface can be wiped or covered with them. Such control allows for the non-invasive in situ detection of analytes [21]. In recent years, lightweight and wearable SERS substrates have been designed that can be equipped with a portable Raman instrument [22] and smartphone [23]. Sun et al. [20] designed flexible SERS substrates containing silver nanoparticles (AgNPs) loaded on PDMS using template lithography. Sandpaper of various roughnesses was utilized as a template to deposit AgNPs on the PDMS substrate. By optimizing the lading of AgNPs, they could detect a model dye, Rhodamine 6G (R6G), at four femto moles. This AgNP-loaded PDMS substrate allowed for Raman enhancement and provided direct sampling capability. This substrate detected pesticides placed on cherry tomatoes at the ng level. Das and co-workers [24], attached AgNPs on unaltered filter papers following the classic "silver-mirror" experiment. The AgNP–filter paper substrates allowed for SERS detection up to picomolar (10^{-12} M) and nanomolar (10^{-9} M) concentrations for rhodamine 6G and rhodamine B, respectively. The observed enhancement factors (EFs) for these measurements were 1.42×10^{10} and 0.659×10^{6}, respectively. Liu et al. [25] fabricated AgNP-immobilized cotton swabs with the help of polydopamine (PDA) to detect bactericide residues rapidly on fruits, vegetables, and crops. Dithiocarbamate bactericide, known as thiram, is frequently used to prevent the fungal infection of crops, fruits, and vegetables. To create this substrate, the precleaned cotton swabs were dipped in DA, which was then self-polymerized to create PDA. Later, the AgNPs were grown on the PDA-modified cotton swabs by reducing Ag^+ ions by catechol on PDA. Jiang and co-workers [26] devised a technique where analytes were collected by using flexible transparent adhesive tapes with subsequent pasting on a SERS substrate of an Al_2O_3-coated silver nanorod array. This rapid technique is based on the "tape-wrapped SERS" and paste, peel off, and paste again method. This method allowed the researchers to obtain distinct SERS signals of pesticides like thiabendazole and tetramethylthiuram disulfide from the surfaces of fruits and vegetables. This technique demonstrated tremendous potential for application in environmental monitoring and food safety.

This study presents a simple method of immobilizing AgNP on cotton fabrics (CF) to create a flexible, cost-effective, portable, and sensitive SERS substrate, AgNP@CF. Commercially available cotton fabric contains -OH groups. In a pretreatment process, deprotonate -OH groups and Ag^+ ions were allowed to bind. In the consecutive step, the Ag^+ ions were reduced to fiber-bound AgNPs, generating AgNP@CF. Three different AgNP@CF composites were created, varying the concentration of the precursor $AgNO_3$ solution. The AgNP@CF composites were characterized by SEM, EDX, XRD, and FTIR spectroscopy. We assessed the SERS capability of these AgNP@CF composites by using melamine (Mela) as a model compound. Melamine is primarily used for the production of thermosetting plastic and as raw material to produce synthetic polymer. It is an odorless and tasteless nitrogen-rich molecule, and it has been illegally added to infant formula and pet food to falsify the high protein content based on nitrogen [27], and that attracted significant attention to the SERS detection of melamine. Many kidney infections and even deaths in infants and pets have been reported due to melamine ingestion [27]. We explored melamine detection with the designed SERS substrates by dipping them in a desired concentration of aqueous melamine solution

2. Results and Discussion

In this work, we demonstrated the in situ production of AgNP on CF. Using a standard method, CF was first cleaned with a boiled solution of a strong base and surfactant. Before immobilization, the Ag^+ ions on the -OH of the cellulose fibers CF were pretreated with KOH with a subsequent rinse of DI water. The process allowed the Ag^+ ions to attach to the CF fibers electrostatically while soaked in an $AgNO_3$ solution. The immobilized Ag^+ ions were later reduced to immobilized AgNP with ascorbic acid as a reducing agent [28]. The synthetic route is represented in Scheme 1.

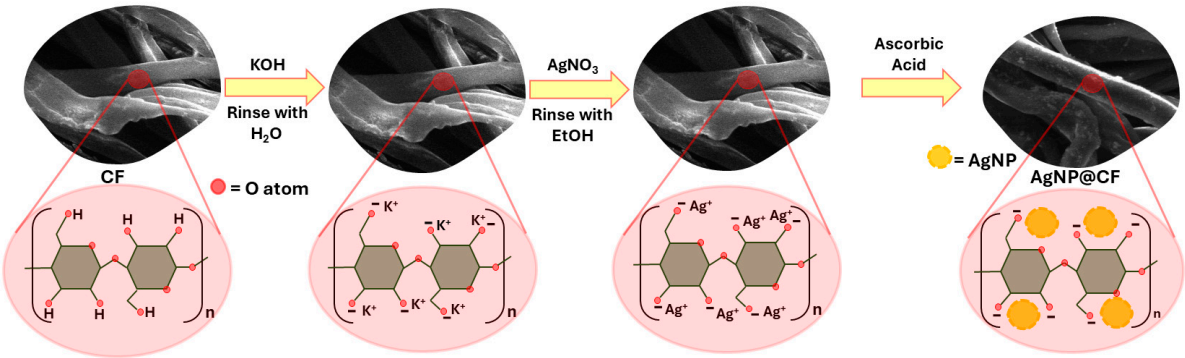

Scheme 1. Schematic representation of in situ synthesis of AgNP on CF creating AgNP@CF composite.

2.1. SEM and EDX Analysis of AgNP@CF Composites

The scanning electron microscopic (SEM) morphologies and digital pictures of the empty CF and composites AgNP@CF-1, AgNP@CF-2, and AgNP@CF-3 are shown in Figure 1. The digital images indicate that the empty CF was modified with AgNP, and the AgNP-immobilized CF was yellowish brown. The SEM images further confirm that the individual fibers were loaded with AgNPs (Figure 1). The AgNP immobilization did not degrade the integrated woven structure of the CF.

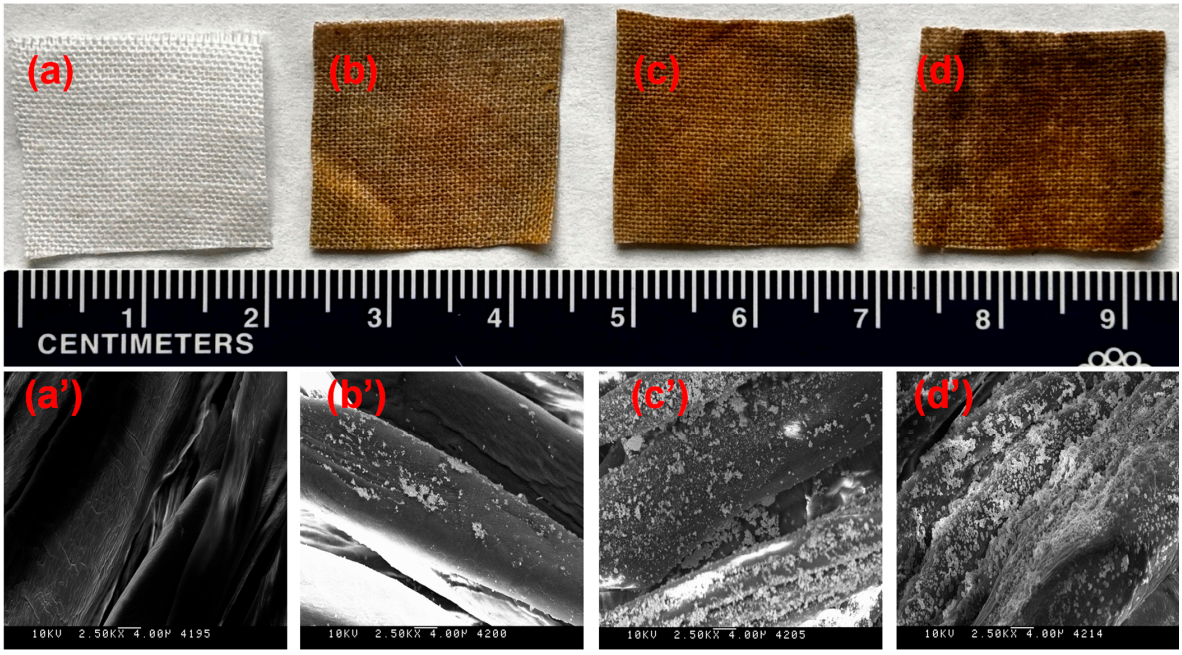

Figure 1. Digital photographs of empty CF (**a**), AgNP@CF-1 (**b**), AgNP@CF-2 (**c**), and AgNP@CF-3 (**d**) are shown (sample size: ~2 cm × ~2 cm). Corresponding SEM images of empty CF (**a'**), AgNP@CF-1 (**b'**), AgNP@CF-2 (**c'**), and AgNP@CF-3 (**d'**) are also shown (scale bar 4 µm). Images were taken with Topcon DS-130F Field-Emission Scanning Electron Microscope at operating voltage of 10 kV.

The EDX analysis indicated the presence of all the elemental components of the empty CF, AgNP@CF-1, AgNP@CF-2, and AgNP@CF-3, as shown in Figure 2. Signals at 0.27 and 0.51 keV indicate the presence of carbon and carbon, respectively. These signals are present in all the samples and attributed to cellulose. The absorption peaks at 2.98, 3.16, and 3.34 keV indicate Ag (L_{alpha}), Ag (L_{beta}), and Ag (L_{beta2}) signals, respectively [29]. The presence of these signals in all three AgNP@CF composites confirms the immobilization of silver nanoparticles. The signal at 8.06 keV is due to Cu tape used for the SEM-EDX measurement to mount the sample [19].

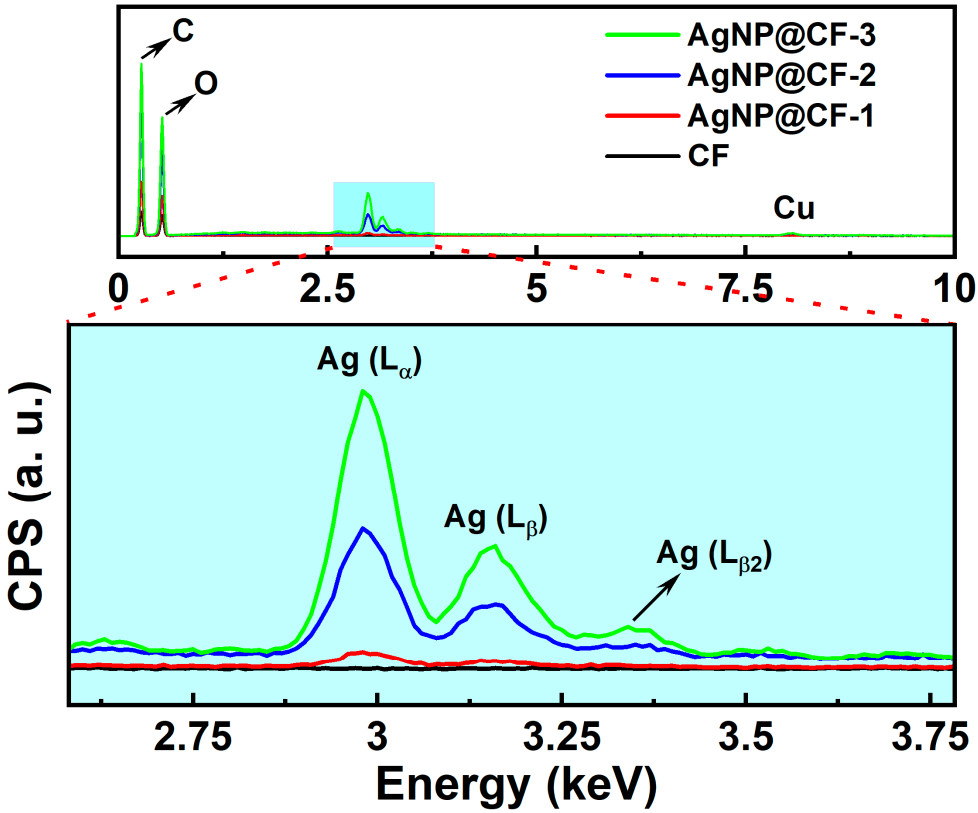

Figure 2. The EDX spectra of empty CF (black line), AgNP@CF-1 (red line), AgNP@CF-2 (blue line), and AgNP@wipe-3 (green line) are shown here and confirm the presence of silver in the AgNP@CF composites. Analysis was conducted using a VEGA3 TESCAN at an operating voltage of 30 kV.

2.2. XRD Analysis

We performed XRD analysis on the samples to check the crystallinity of the CF, AgNP@C-1, AgNP@CF-2, and AgNP@CF-3. The XRD signals are presented in Figure 3. The bottom black line is for empty CF, and the characteristic signals appear at 2θ values 14.4°, 16.0°, 22.2°, and 33.7°, respectively, corresponding to the (1 1 0), (1 1 0), (2 0 0), and (0 0 4) planes [30]. It is indicative of the presence of cellulose I crystal structure. The three composites AgNP@C-1, AgNP@CF-2, and AgNP@CF-3 exhibit those four lines of cellulose but are progressively shifted due to their bonding to the metal nanoparticles (Figure 3). For AgNP@CF-3, the signals appear at 2θ values 15.3°, 16.9°, 22.9°, and 34.5°. The shift is, respectively, 0.9°, 0.9°, 0.7°, and 0.8° compared to the CF sample. The composite AgNP@C-1 has one additional signal at 2θ values 37.8° indexed to the (1 1 1) plane of Ag. The composite AgNP@C-2 has four characteristic peaks at 2θ values 38.1°, 44.2°, 64.4°, and 77.1° which are indexed to the (1 1 1), (2 0 0), (2 2 0), and (3 1 1) planes [31]. The composite AgNP@C-3 has four similar but right-shifted signals at 2θ values 38.5°, 44.7°, 64.8°, and 77.7° which are indexed to the (1 1 1), (2 0 0), (2 2 0), and (3 1 1) planes [31]. It indicates that the synthesized nanoparticles are pure crystalline and fcc structure [27].

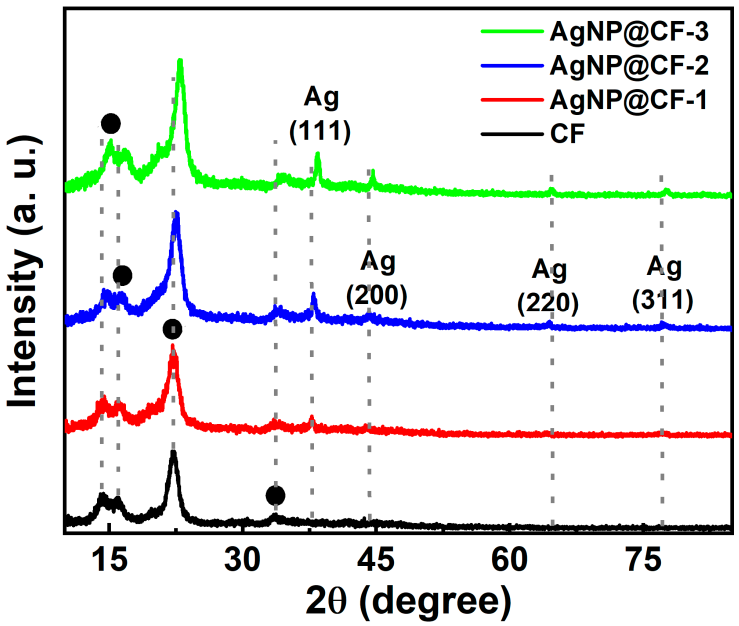

Figure 3. XRD patterns of empty CF (black line), AgNP@CF-1 (red line), AgNP@CF-2, (blue line), and AuNP@CF-3 (green line). The signals of cotton fabric are identified with a black circle. The silver signals are also identified wherever visible.

2.3. The Characterization of the AgNP@CF Composites by FTIR Spectroscopy

In Figure 4, we plot the FTIR spectra of empty CF, AgNP@CF-1, AgNP@CF-2, and AgNP@CF-3. For the latter three, $AgNO_3$ concentrations were 10.0 mM, 25.0 mM, and 50.0 mM, respectively, during the in situ synthesis. The empty CF shows signals at 3287–3333, 2862–2899, 1300–1470, and 970–1250 cm^{-1} that are assigned to O-H stretch, C-H stretch, asymmetric C-H and O-H bending, and C-O stretching, respectively. As is evident from the SEM image, the entire surface of the CF fibers is not covered by AgNP in the above three composites. As a result, the FTIR spectra of AgNP@CF-1, AgNP@CF-2, and AgNP@CF-3 composites are reasonably similar to the CF. However, the AgNP will have an affinity towards the O-atoms in the C-O bond. Hence, due to the interaction of the AgNP with the C-O bond, the signals 970–1250 cm^{-1} are significantly broadened (Figure 4 and Scheme 1).

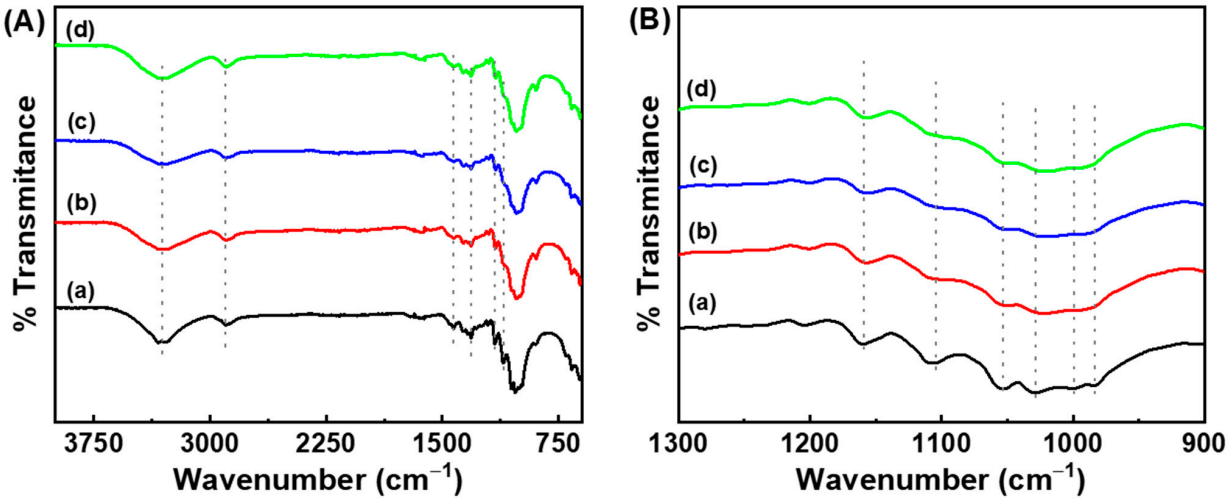

Figure 4. In both (**A**,**B**), FTIR spectra of empty CF (a, black line), AgNP@CF-1 (b, red line), AgNP@CF-2 (c, blue line), and AgNP@CF-3 (d, green line) composites are shown.

2.4. Raman Spectroscopy and AgNPs@CF as SERS Substrate

This report explores melamine as our model analyte and probes it with Raman spectroscopy and SERS. Melamine is a food contaminant that causes trouble for both infant and pet food [32]. First, we studied the Raman spectra of solid melamine, 25 mM melamine, 10 mM melamine, and 1.0 mM melamine, as shown in Figure 5. As depicted in Figure 5, the Raman spectrum of melamine has two characteristic signals, namely, trigonal ring breathing modes at 677 cm^{-1} (>C-NH_2) and 984 cm^{-1} (>C-N=C<). Melamine solutions of 1.0, 10, and 25 mM did not show any signal due to the weak nature of the Raman technique.

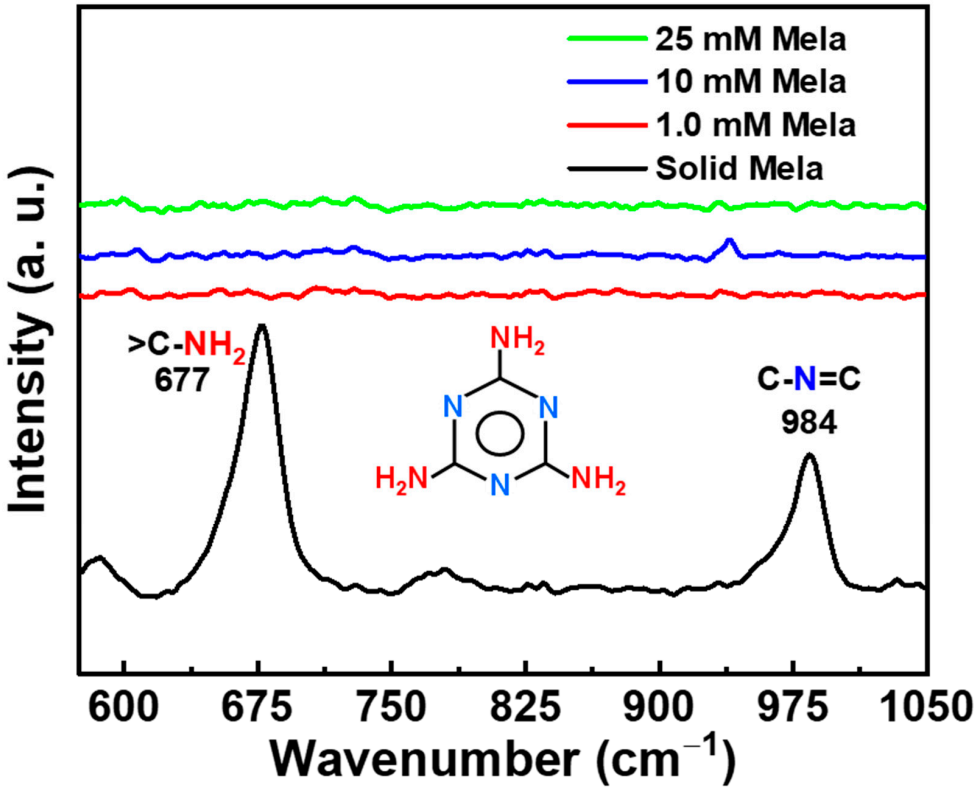

Figure 5. Raman spectra of solid melamine (black line), 1.0 mM melamine (red line), 10 mM melamine (blue line), and 25 mM melamine (green line).

In Figure 6, the SERS signals of melamine adsorbed on composites AgNP@CF-1, AgNP@CF-2, and AgNP@CF-3 are significantly enhanced. We varied the concentrations of the melamine solutions from 0.1 to 1.0 to 5.0 mM. The composites soaked in the above melamine solutions show progressive signal enhancement in the following order: AgNP@CF-1 < AgNP@CF-2 < AgNP@CF-3. Composites with higher AgNP concentrations have the highest intensity. In addition, the composite soaked in higher melamine concentration adsorbs more melamine and represents higher signal intensity (Figure 6). It is worth noting that only >C-NH_2 ring breathing signal intensity becomes enhanced during the SERS measurement. As the lone pair on the -NH_2 group has a higher affinity towards the silver nanoparticle surface, those groups are in the vicinity of the nanometal surface or possibly bind the metal surface. Because of this, the interaction of the SERS signal has been shifted by 9–23 cm^{-1}, going from the Raman spectrum of 100 mM melamine to the SERS spectra of AgNP@CF composites, as shown in Table 1.

As demonstrated in Table 1, the *SERS* analytical enhancement factor (AEF) was calculated based on the relative sample concentrations and signal intensities. Measurement was made based on the ratio of *SERS* intensity for the selected mode of a given analyte intensity (I_{SERS}) and the corresponding Raman intensity (I_{RS}) under identical experimental

conditions (e.g., laser wavelength, laser power, integration time, sample preparation, etc.) using the following equation [33]:

$$\mathrm{AEF} = \frac{I_{SERS}}{I_{RS}} \frac{C_{RS}}{C_{SERS}} \quad (1)$$

Equation (1) represents C_{RS} and C_{SERS}, which are the respective concentrations of the analyte in the Raman and *SERS* experiments. As indicated in Figure 6, we calculated all AEFs based on the Raman spectrum of the 100 mM melamine solution. The concentrations where the AgNP@CF composites are soaked before *SERS* measurements are 5.0, 1.0, and 0.1 mM melamine (Figure 6). The data presented in Table 1 are calculated based on constant C_{RS} = 0.1 M. There are three as follows: $C_{SERS} = 5.0 \times 10^{-3}$ M, $C_{SERS} = 1.0 \times 10^{-3}$ M, and $C_{SERS} = 1.0 \times 10^{-4}$ M. The relative I_{RS} and I_{SERS} intensities are calculated from the spectra shown in Figure 6. The AEF values presented in Table 1 lie within the reasonable AEF values reported in the literature [34].

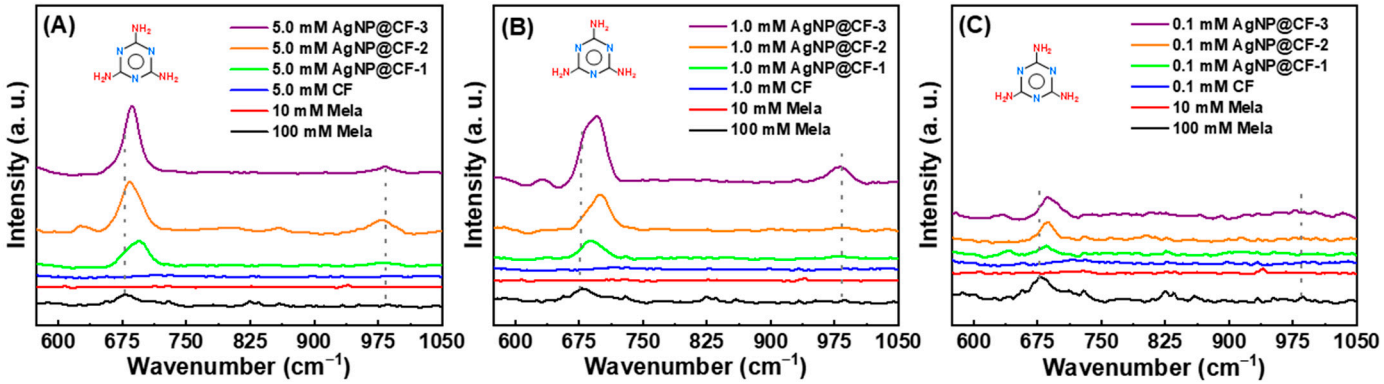

Figure 6. Raman spectra of 100 mM melamine (black line) and 10 mM melamine (red line) for (**A**–**C**). Raman spectra of CF soaked in 5.0 mM (**A**), 1.0 mM (**B**), and 0.1 mM melamine (blue line). SERS spectra of AgNP@CF-1 (green line), AgNP@CF-2 (orange line), and AgNP@CF-3 (purple line) for (**A**–**C**). AgNP@CF-1, AgNP@CF-2, and AgNP@CF-3 were soaked in 5.0 mM (**A**), 1.0 mM (**B**), and 0.1 mM of melamine prior to SERS measurements.

Table 1. The *SERS* analytical enhancement factor (AEF) for three different composite materials considering the Raman signal at 677 cm^{-1} at three different melamine concentrations.

Samples	Raman (cm^{-1})	SERS (cm^{-1})	AEF (5.0 mM)	SERS (cm^{-1})	AEF (1.0 mM)	SERS (cm^{-1})	AEF (0.1 mM)
100 mM	677	-	-	-	-	-	-
AgNP@CF-1	-	694	$0.45 \times 10^2 \pm 2.2$	689	$1.35 \times 10^2 \pm 3.0$	685	$4.45 \times 10^2 \pm 34$
AgNP@CF-2	-	684	$0.84 \times 10^2 \pm 2.3$	700	$2.58 \times 10^2 \pm 3.0$	687	$8.15 \times 10^2 \pm 24$
AgNP@CF-3	-	686	$1.17 \times 10^2 \pm 2.8$	696	$4.73 \times 10^2 \pm 9.5$	687	$9.18 \times 10^2 \pm 30$

The limit of detection (LOD) of melamine using various SERS substrates is compared with the results in this report, as shown in Table 2. In most of the results compared in this report, the SERS substrates are not immobilized on the solid surface. However, a few of them were immobilized on non-flexible solid surfaces, and one of them was immobilized on non-woven fibers. These data show that the suspended substrates have a better LOD than the immobilized ones, and among the immobilized ones, the one with the flexible substrate had a relatively low LOD. This last substrate, which contains baby wipes and AgNP, was designed in the Baruah laboratory [19]. Compared to our previous results with AgNP@wipe [19], the current substates of AgNP@CF have a better LOD. We are creating other flexible SERS substrates. The work is in progress, and we hope to improve the LOD further with such flexible SERS substrates.

Table 2. A comparison of the limit of detection (LOD) of melamine in molar concentrations using various SERS substrates.

Sl. #	SERS Substrate	LOD (M)	Reference
1	Ag nanocube	7.9×10^{-8}	[35]
2	Ag/C/AgNps	5.0×10^{-8}	[33]
3	CS-ATS-Ag cotton swabs	1.6×10^{-6}	[27]
4	MEL-T31-AgNPs	7.9×10^{-7}	[36]
5	Fern-like silver nanodendrites (AgNDs)	1.6×10^{-7}	[37]
6	Ag colloid	8.0×10^{-3}	[38]
7	Starch-coated AgNPs	1.6×10^{-8}	[39]
8	Silver dendrite	7.9×10^{-4}	[40]
9	$Ag/SiO_2/Au/Si$ substrate	1.0×10^{-9}	[41]
10	CD-AgNPs	2.4×10^{-8}	[42]
11	AgNP@wipe	1.0×10^{-3}	[19]
12	AgNP@CF	1.0×10^{-4}	This work

3. Materials and Methods

3.1. Materials

$AgNO_3$ (99%) was purchased from Sigma-Aldrich, St. Louis, MO, USA; ascorbic acid (99%) and melamine (98.0%) were purchased from Across Organic; sodium hydroxide, potassium hydroxide, and sodium citrate dihydrate were purchased from Fisher Scientific, Suwanee, GA, USA; Triton X-100 was purchased from VWR analytics, Radnor, PA, USA; 100% cotton fabrics were purchased from Walmart, Woodstock, GA, USA. All chemicals and solvents were used without further purification. All glassware was cleaned with aqua regia (3:1 v/v HCl (37%)/HNO_3 (65%) solutions) and then rinsed thoroughly with DI H_2O before use. Caution: aqua regia solutions are dangerous and highly corrosive. This should be used with extreme care. Fresh aqua regia solutions should not be stored in closed containers. The DI water in all experiments was Milli-Q water (18 MΩ cm, Millipore, Burlington, MA, USA).

3.2. The Precleaning of the Cotton Fabrics

A detergent solution was used to scour the cotton fabrics to remove all residual chemicals prior to activating and depositing the silver nanoparticles onto the fibers [43]. A total of 25.0 g of solid sodium hydroxide (NaOH), 7.5 g of Triton X-100, and 3.75 g of sodium citrate were dissolved in 500 mL of deionized water. Two pieces of 10 cm × 10 cm cotton fabrics were stirred in this solution at 100 °C for 1 h then rinsed with excess deionized water several times. All cotton fabrics were then air-dried.

3.3. In situ Synthesis of AgNPs on Cotton Fabrics

The dried cotton fabric samples were cut into 2 cm × 2 cm pieces for silver nanoparticle deposition. As shown in Scheme 1, such cotton fabrics were first thoroughly immersed in 100 mL of 6 M potassium hydroxide (KOH) for 5 min at room temperature, then rinsed several times with deionized water. All fabrics were kept in a wet state until the next step in treatment. Such treatment deprotonates the cellulosic hydroxyl groups creating "-O^- K^+" moiety [44], as depicted in Scheme 1. Six pieces of pretreated cotton fabrics (2 cm × 2 cm) were immersed in 50 mL of $AgNO_3$ solutions with a $AgNO_3$ concentration of 10 mM or 25 mM or 50 mM for 30 min. Ag^+ ions became impregnated into the cellulose fibers now replacing the K^+ ions forming "-O^- Ag^+" moiety [44]. Then, the cotton fabrics were rinsed with ethanol to remove un-bound Ag^+ ions. After that. the Ag^+-impregnated cotton fabric was immersed into 25 mL of 10 mM ascorbic acid solution for 15 min and then rinsed with DI water. The colorless cotton fabrics turned dark yellow (see Figure 1).

3.4. FTIR Studies of AgNP Composites

FTIR spectroscopy was performed using a Perkin-Elmer FTIR Spectra 100 spectrometer fitted with diamond ATR (PerkinElmer, Inc., Waltham, MA, USA). The spectra were further processed and plotted with OriginPro 2020b, version 9.7.5(Academic) software.

3.5. Raman Spectroscopic Measurement

One piece of the dried AgNP@CF composite was immersed in a 5.0 mM, 1.0 mM, or 0.1 mM aqueous solution of melamine for 30 min to form an adsorbed layer on the substrate. After rinsing off the un-adsorbed melamine molecules with water, SERS spectra were measured. The analyte-adsorbed AgNP@CF composite was stuffed in glass sample vials for the SERS measurement. Raman spectroscopic measurements were carried out on a DeltaNu Advantage 200 A Raman spectrometer equipped with a HeNe laser set at 633 nm with an integration time of 10.0 s.

3.6. SEM and EDX Analysis

SEM data were collected using a Topcon DS150 Field-Emission Scanning Electron Microscope (FESEM, JEOL, Tokyo, Japan) at 10 kV in secondary electron mode. SEM on the microplastics was conducted using a VEGA3 TESCAN (TESCAN, Brno, Czech Republic) at 30 kV. The VEGA3 TESCAN was equipped with a Thermo-Fisher Scientific EDX spectrometer (Thermo-Fisher Scientific, Waltham, MA, USA). The EDX has software, Pathfinder 2.11, with a database of reference spectra for elemental analysis and mapping. Small pieces of CF and AgNP@CF composites were fixed on an aluminum stage with the help of double-sided copper tape and introduced into the chamber.

3.7. XRD Analysis

An XRD analysis of the cleaned cotton fabric and the corresponding composite materials was recorded with a Rigaku miniflex X-ray diffractometer (Tokyo, Japan, Cu Kα, 40 kV, 15 mA) from 5° to 90° (2θ) at a scanning speed of 5°/min.

4. Conclusions

In conclusion, the silver nanoparticles were successfully immobilized onto the fibers of cotton fabrics by way of in situ synthesis. Three different silver nitrate concentrations (10 mM, 25 mM, and 50 mM) were used to create the composite materials: AgNP@CF-1, AgNP@CF-2, and AgNP@CF-3. These were characterized by SEM, EDX analysis, XRD, and FTIR spectroscopy.

It is evident in the literature that immobilizing nanomaterials on rigid substances like glass and silicon wafers [16,17] yields excellent *SERS* substrates. However, such rigid surfaces have one critical drawback: they are incompetent to acquire samples from real-world surfaces. For example, in the SERS detection of explosives in an airport setting, rigid SERS substrates would be inconvenient and ineffective [45]. The SERS substrates of glass, silicon, and alumina are inelastic, delicate, and useless for collecting samples from everyday surfaces [45]. However, flexible SERS substrates like the one reported in the current report, AgNP@CF, have a significant advantage in collecting trace amounts of analytes from real-life surfaces. A food contaminant/toxin, melamine, was used to probe the SERS capabilities of the fabricated composites. Before SERS measurements, each of those three composites, AgNP@CF-1, AgNP@CF-2, and AgNP@CF-3, were soaked in 5.0 mM, 1.0 mM, or 0.1 mM melamine solutions. The SERS data indicated that the >C-NH_2 ring breathing signal at 677 cm^{-1} intensity becomes enhanced, while the other signal at 984 cm^{-1} (>C-N=C<) does show only minimal enhancement. As the lone pair on the -NH_2 group has a higher affinity towards the silver nanoparticle surface, those groups are in the vicinity of the nanometal surface or possibly bind the metal surface. Because of this, the interaction of the SERS signal has also been right-shifted by 9–23 cm^{-1}. The SERS data show the progressive signal enhancement in the following order: AgNP@CF-1 < AgNP@CF-2 < AgNP@CF-3. Finally, the calculated SERS AEF lies within the reasonable AEF values reported in the literature.

The SERS substrate AgNP@CF is composed of flexible fibers and AgNP and has certain advantages over other flexible SERS substrates. The cotton fabric, being a porous material, has micro- and nanocavities, a moderately robust structure, and an abundance of -OH groups that facilitate the facile immobilization of AgNPs. The conversion of attached silver ions to AgNP can be achieved following a simple green synthetic method with ascorbic acid as a reducing agent. The composite material, AgNP@CF, thus created, is a flexible, non-invasive, cost-effective, eco-friendly composite as a SERS substrate.

Author Contributions: Conceptualization, B.B.; Methodology, B.B.; Formal analysis, B.B. and M.W.; Investigation, B.B. and M.W.; Data curation, B.B.; Writing—original draft, B.B.; Visualization, B.B.; Supervision, B.B.; Project administration, B.B.; Funding acquisition, B.B. All authors have read and agreed to the published version of the manuscript.

Funding: This work was supported by Kennesaw State University, Department of Chemistry and Biochemistry, KSU CSM Mentor Protégé fund (BBaruah-01-FY2015-01) and KSU FY 2015 OVPR pilot/seed grant awarded to Bharat Baruah.

Data Availability Statement: The original contributions presented in the study are included in the article, further inquiries can be directed to the corresponding author.

Acknowledgments: We acknowledge Robert P. Apkarian Integrated Electron Microscopy Core at Emory University for STEM analysis and Advanced Materials Research Laboratories (AMRL) at Clemson University for STEM and EDX analysis.

Conflicts of Interest: The authors declare that they have no conflict of interest.

References

1. Singh, J.; Mehta, A. Rapid and sensitive detection of mycotoxins by advanced and emerging analytical methods: A review. *Food Sci. Nutr.* **2020**, *8*, 2183–2204. [CrossRef] [PubMed]
2. Malečková, M.; Vrzal, T.; Olšovská, J. Development of a method for melamine determination in beer and beer-type beverages by GC-MS/MS. *Kvasny Prum.* **2020**, *66*, 331. [CrossRef]
3. Zhou, Q.; Tan, X.C.; Guo, X.J.; Huang, Y.J.; Zhai, H.Y. Preparation and characterization of molecularly imprinted solid-phase extraction column coupled with high-performance liquid chromatography for selective determination of melamine. *R. Soc. Open Sci.* **2018**, *5*, 180750. [CrossRef]
4. Sushma, U.; Srivastava, K.A.; Krishnan, H.M. Melamine Detection in Food matrices employing Chicken Antibody (IgY): A Comparison between Colorimetric and Chemiluminescent Methods. *Curr. Anal. Chem.* **2019**, *15*, 668–677. [CrossRef]
5. de Koning, S.; Janssen, H.-G.; Brinkman, U.A.T. Modern Methods of Sample Preparation for GC Analysis. *Chroma* **2009**, *69*, 33–78. [CrossRef]
6. Domínguez, I.; Garrido Frenich, A.; Romero-González, R. Mass spectrometry approaches to ensure food safety. *Anal. Methods* **2020**, *12*, 1148–1162. [CrossRef]
7. Miseo, E.V.; Bradley, M.S. 2022 Review of spectroscopic instrumentation. *Spectroscopy* **2022**, *37*, 40–54. [CrossRef]
8. Schulz, H.; Baranska, M. Identification and quantification of valuable plant substances by IR and Raman spectroscopy. *Vib. Spectrosc.* **2007**, *43*, 13–25. [CrossRef]
9. Langer, J.; Jimenez de Aberasturi, D.; Aizpurua, J.; Alvarez-Puebla, R.A.; Auguié, B.; Baumberg, J.J.; Bazan, G.C.; Bell, S.E.J.; Boisen, A.; Brolo, A.G.; et al. Present and Future of Surface-Enhanced Raman Scattering. *ACS Nano* **2020**, *14*, 28–117. [CrossRef]
10. Zhang, D.; Pu, H.; Huang, L.; Sun, D.-W. Advances in flexible surface-enhanced Raman scattering (SERS) substrates for nondestructive food detection: Fundamentals and recent applications. *Trends Food Sci. Technol.* **2021**, *109*, 690–701. [CrossRef]
11. Wang, K.; Sun, D.-W.; Pu, H.; Wei, Q. Shell thickness-dependent Au@Ag nanoparticles aggregates for high-performance SERS applications. *Talanta* **2019**, *195*, 506–515. [CrossRef] [PubMed]
12. Sun, J.; Gong, L.; Wang, W.; Gong, Z.; Wang, D.; Fan, M. Surface-enhanced Raman spectroscopy for on-site analysis: A review of recent developments. *Luminescence* **2020**, *35*, 808–820. [CrossRef] [PubMed]
13. Heleg-Shabtai, V.; Sharabi, H.; Zaltsman, A.; Ron, I.; Pevzner, A. Surface-enhanced Raman spectroscopy (SERS) for detection of VX and HD in the gas phase using a hand-held Raman spectrometer. *Analyst* **2020**, *145*, 6334–6341. [CrossRef] [PubMed]
14. Perumal, J.; Wang, Y.; Attia, A.B.E.; Dinish, U.S.; Olivo, M. Towards a point-of-care SERS sensor for biomedical and agri-food analysis applications: A review of recent advancements. *Nanoscale* **2021**, *13*, 553–580. [CrossRef] [PubMed]
15. Huang, T.-C.; Tsai, H.-C.; Chin, Y.-C.; Huang, W.-S.; Chiu, Y.-C.; Hsu, T.-C.; Chia, Z.-C.; Hung, T.-C.; Huang, C.-C.; Hsieh, Y.-T. Concave Double-Walled AgAuPd Nanocubes for Surface-Enhanced Raman Spectroscopy Detection and Catalysis Applications. *ACS Appl. Nano Mater.* **2021**, *4*, 10103–10115. [CrossRef]

16. Li, C.; Huang, Y.; Li, X.; Zhang, Y.; Chen, Q.; Ye, Z.; Alqarni, Z.; Bell, S.E.J.; Xu, Y. Towards practical and sustainable SERS: A review of recent developments in the construction of multifunctional enhancing substrates. *J. Mater. Chem. C* **2021**, *9*, 11517–11552. [CrossRef]
17. Yaseen, T.; Pu, H.; Sun, D.-W. Effects of Ions on Core-Shell Bimetallic Au@Ag NPs for Rapid Detection of Phosalone Residues in Peach by SERS. *Food Anal. Methods* **2019**, *12*, 2094–2105. [CrossRef]
18. Zong, C.; Ge, M.; Pan, H.; Wang, J.; Nie, X.; Zhang, Q.; Zhao, W.; Liu, X.; Yu, Y. In situ synthesis of low-cost and large-scale flexible metal nanoparticle–polymer composite films as highly sensitive SERS substrates for surface trace analysis. *RSC Adv.* **2019**, *9*, 2857–2864. [CrossRef] [PubMed]
19. Baruah, B. In situ and facile synthesis of silver nanoparticles on baby wipes and their applications in catalysis and SERS. *RSC Adv.* **2016**, *6*, 5016–5023. [CrossRef]
20. Sun, J.; Gong, L.; Gong, Z.; Wang, D.; Yin, X.; Fan, M. Facile fabrication of a large-area and cost-effective PDMS-SERS substrate by sandpaper template-assisted lithography. *Anal. Methods* **2019**, *11*, 4917–4922. [CrossRef]
21. Li, D.; Zhu, Z.; Sun, D.-W. Visualization of the in situ distribution of contents and hydrogen bonding states of cellular level water in apple tissues by confocal Raman microscopy. *Analyst* **2020**, *145*, 897–907. [CrossRef] [PubMed]
22. Sun, M.; Li, B.; Liu, X.; Chen, J.; Mu, T.; Zhu, L.; Guo, J.; Ma, X. Performance enhancement of paper-based SERS chips by shell-isolated nanoparticle-enhanced Raman spectroscopy. *J. Mater. Sci. Technol.* **2019**, *35*, 2207–2212. [CrossRef]
23. Zeng, F.; Duan, W.; Zhu, B.; Mu, T.; Zhu, L.; Guo, J.; Ma, X. Paper-Based Versatile Surface-Enhanced Raman Spectroscopy Chip with Smartphone-Based Raman Analyzer for Point-of-Care Application. *Anal. Chem.* **2019**, *91*, 1064–1070. [CrossRef] [PubMed]
24. Das, D.; Senapati, S.; Nanda, K.K. "Rinse, Repeat": An Efficient and Reusable SERS and Catalytic Platform Fabricated by Controlled Deposition of Silver Nanoparticles on Cellulose Paper. *ACS Sustain. Chem. Eng.* **2019**, *7*, 14089–14101. [CrossRef]
25. Liu, J.; Si, T.; Zhang, L.; Zhang, Z. Mussel-Inspired Fabrication of SERS Swabs for Highly Sensitive and Conformal Rapid Detection of Thiram Bactericides. *Nanomaterials* **2019**, *9*, 1331. [CrossRef] [PubMed]
26. Jiang, J.; Zou, S.; Ma, L.; Wang, S.; Liao, J.; Zhang, Z. Surface-Enhanced Raman Scattering Detection of Pesticide Residues Using Transparent Adhesive Tapes and Coated Silver Nanorods. *ACS Appl. Mater. Interfaces* **2018**, *10*, 9129–9135. [CrossRef]
27. Huang, W.C.; Cheng, K.F.; Shyu, J.Y. Flexible SERS substrate of silver nanoparticles on cotton swabs for rapid in situ detection of melamine. *Nanoscale Adv.* **2022**, *4*, 1164–1172. [CrossRef]
28. Qin, Y.; Ji, X.; Jing, J.; Liu, H.; Wu, H.; Yang, W. Size control over spherical silver nanoparticles by ascorbic acid reduction. *Colloids Surf. A* **2010**, *372*, 172–176. [CrossRef]
29. Phongtongpasuk, S.; Poadang, S.; Yongvanich, N. Environmental-friendly Method for Synthesis of Silver Nanoparticles from Dragon Fruit Peel Extract and their Antibacterial Activities. *Energy Procedia* **2016**, *89*, 239–247. [CrossRef]
30. Andra, S.; Balu, S.K.; Jeevanandam, J.; Muthalagu, M.; Danquah, M.K. Surface cationization of cellulose to enhance durable antibacterial finish in phytosynthesized silver nanoparticle treated cotton fabric. *Cellulose* **2021**, *28*, 5895–5910. [CrossRef]
31. Diwakar, B.S.; Govindh, B.; Sekhar, D.C.; Bhavani, P.; Swaminadham, V.; Reddy, K.A. Room temperature dielectric and antibacterial behavior of thiosemicarbazide capped low dimension Silver and Gold nanoparticles. *Int. J. Nano Dimens.* **2017**, *8*, 274–283.
32. Huang, H.; Shende, C.; Sengupta, A.; Inscore, F.; Brouillette, C.; Smith, W.; Farquharson, S. Surface-enhanced Raman spectra of melamine and other chemicals using a 1550 nm (retina-safe) laser. *J. Raman Spectrosc.* **2012**, *43*, 701–705. [CrossRef]
33. Chen, L.-M.; Liu, Y.-N. Surface-Enhanced Raman Detection of Melamine on Silver-Nanoparticle-Decorated Silver/Carbon Nanospheres: Effect of Metal Ions. *ACS Appl. Mater. Interfaces* **2011**, *3*, 3091–3096. [CrossRef]
34. Le Ru, E.C.; Blackie, E.; Meyer, M.; Etchegoin, P.G. Surface Enhanced Raman Scattering Enhancement Factors: A Comprehensive Study. *J. Phys. Chem. C* **2007**, *111*, 13794–13803. [CrossRef]
35. Li, L.; Chin, W.S. Rapid and sensitive SERS detection of melamine in milk using Ag nanocube array substrate coupled with multivariate analysis. *Food Chem.* **2021**, *357*, 129717. [CrossRef] [PubMed]
36. Xing, H.; Zheng, B.; Li, X.; Dang, X.; Zhang, H.; Tian, F.; Hu, X. Sensitive SERS detection of melamine and cyromazine in raw milk using aptamer-based in situ silver nanoparticles synthesis. *Results Chem.* **2022**, *4*, 100266. [CrossRef]
37. Cuong, N.M.; Cao, D.T.; Thu, V.T.; Ngan, L.T.-Q. Direct detection of melamine in liquid milk and infant formula using surface-enhanced Raman scattering combined with silver nanodendrites. *Optik* **2021**, *243*, 167504. [CrossRef]
38. Chen, X.; Hu, Y.; Gao, J.; Zhang, Y.; Li, S. Interaction of Melamine Molecules with Silver Nanoparticles Explored by Surface-Enhanced Raman Scattering and Density Functional Theory Calculations. *Appl. Spectrosc.* **2013**, *67*, 491–497. [CrossRef] [PubMed]
39. Zhao, Y.; Tian, Y.; Ma, P.; Yu, A.; Zhang, H.; Chen, Y. Determination of melamine and malachite green by surface-enhanced Raman scattering spectroscopy using starch-coated silver nanoparticles as substrates. *Anal. Methods* **2015**, *7*, 8116–8122. [CrossRef]
40. Li, X.; Feng, S.; Hu, Y.; Sheng, W.; Zhang, Y.; Yuan, S.; Zeng, H.; Wang, S.; Lu, X. Rapid Detection of Melamine in Milk Using Immunological Separation and Surface Enhanced Raman Spectroscopy. *J. Food Sci.* **2015**, *80*, C1196–C1209. [CrossRef]
41. Wang, Z.; Liu, J.; Wang, J.; Ma, Z.; Kong, D.; Jiang, S.; Luo, D.; Liu, Y.J. Graphene Oxide-Coated Metal–Insulator–Metal SERS Substrates for Trace Melamine Detection. *Nanomaterials* **2022**, *12*, 1202. [CrossRef]
42. Athauda, T.J.; Hari, P.; Ozer, R.R. Tuning Physical and Optical Properties of ZnO Nanowire Arrays Grown on Cotton Fibers. *ACS Appl. Mater. Interfaces* **2013**, *5*, 6237–6246. [CrossRef]

43. He, J.; Kunitake, T.; Nakao, A. Facile In Situ Synthesis of Noble Metal Nanoparticles in Porous Cellulose Fibers. *Chem. Mater.* **2003**, *15*, 4401–4406. [CrossRef]
44. Ma, P.; Liang, F.; Sun, Y.; Jin, Y.; Chen, Y.; Wang, X.; Zhang, H.; Gao, D.; Song, D. Rapid determination of melamine in milk and milk powder by surface-enhanced Raman spectroscopy and using cyclodextrin-decorated silver nanoparticles. *Microchim. Acta* **2013**, *180*, 1173–1180. [CrossRef]
45. Lee, C.H.; Tian, L.; Singamaneni, S. Paper-Based SERS Swab for Rapid Trace Detection on Real-World Surfaces. *ACS Appl. Mater. Interfaces* **2010**, *2*, 3429–3435. [CrossRef]